

THE RELATION BETWEEN PREEXISTING DEFECTS AND CHARGING-UP IN 9mol%Y₂O₃-ZrO₂ STUDIED BY AUGER ELECTRON SPECTROSCOPY

GUO HAN-SHENG(郭汉生)[†]

School of Materials Science and Engineering, Beijing Polytechnic University, Beijing 100022, China

W. MAUS-FRIEDRICHS and V. KEMPTER

*Physikalisches Institut der Technischen Universität Clausthal, Leibnizstr. 4
38678 Clausthal-Zellerfeld, Germany*

(Received 8 April 1999)

Electron beam damage and charging process in 9mol%Y₂O₃-stabilized zirconia (YS-ZrO₂) are studied by Auger electron spectroscopy (AES). Electron bombardment induces electron-stimulated desorption at the surface on one hand; on the other hand, it modifies the preexisting defects in the irradiated zone. Both effects will lead to charging-up of YS-ZrO₂. The charging related to the first effect can be compensated by an O₂ environment of 6.5×10⁻⁶ Pa, and the charging related to both effects can be inhibited by specimen heating up to 300 °C. However, the modified preexisting defects will not return to their initial states prior to the radiation. Their charging behavior and charge compensation are discussed in the model of the variants of the oxygen vacancies.

PACC: 8280P; 6172C; 7920L

I. INTRODUCTION

Electron beam is widely used in surface analysis as an excitation in Auger electron spectroscopy (AES) and energy-dispersive X-ray analysis (EXD), to image the topography in scanning electron microscopy (SEM), or to determine the surface structure in low energy electron diffraction (LEED). Unfortunately, some effects at the surface of insulating materials are introduced by the bombarding electrons, such as, radiation damage and charging phenomena, which hamper the performance of analysis.

In AES the electron beam with energy lower than 10 keV cannot produce defects by the direct momentum transfer. However, radiolysis process occurs at the surface or within the irradiated zone of many insulating compounds, which results in defects at the surface and/or within the materials. The charging behavior of the defects determines the charging phenomena of the insulating compounds.

We have introduced an O₂ environment into AES on oxides.^[1] We found that a satisfactory compensation of all the irradiation effects on Al₂O₃, observed in AES as charging phenomena, electron-stimulated desorption (ESD) and contamination of the surface from

residual gas, is achieved in 6.5×10⁻⁶ Pa O₂. However, on 9mol%Y₂O₃-stabilized zirconia (YS-ZrO₂), the satisfactory charging compensation has been achieved limitedly, although ESD of oxygen can be compensated in this environmental AES. In this work we use AES to study the electron beam effects on YS-ZrO₂. Efficient performance of AES on YS-ZrO₂ is possible under conditions of being heated in an O₂ environment of 6.5×10⁻⁶ Pa. We suggest that besides the radiation damage at the surface, the preexisting defects, such as oxygen vacancies, are responsible for the charging-up of YS-ZrO₂.

II. EXPERIMENTAL

In this experiment a scanning auger microprobe was used for spot-resolved AES. The system was described in detail elsewhere.^[1] The central electron gun in cylindrical mirror analyzer (CMA) was served to excite Auger electrons, simultaneously, to damage and to charge the sample. The electron beam effects were examined over many hours with Auger spectra. The primary emission was fixed in the experiments; however the primary current density varied with the angle of incidence α , as well as with the primary energy E_p , as indicated in Table 1.

[†]Corresponding author.

Table 1. The primary parameters used in this work.

Primary energies	E_p/keV	1	2	3	5	8
Primary current density	$\alpha = 0^\circ$	0.42	0.64	1.24	3.17	79.62
$J_p/10^{-2} \text{ A}\cdot\text{cm}^{-2}$	$\alpha = 30^\circ$	0.37	0.55	1.08	2.76	68.95
	$\alpha = 60^\circ$	0.22	0.32	0.62	1.59	39.80

The sample is a 9mol% Y_2O_3 -stabilized ZrO_2 plate (~ 1 mm thick). X-ray diffraction shows that the sample is purely cubic with CaF_2 structure. The sample was cleaned in acetone in an ultrasonic bath, then rinsed with distilled water. After transfer into the analysis chamber the sample was sputtered with 2 keV Ar^+ to eliminate adsorbates. The measurements were performed at a polished (100) surface. For charging reduction during AES, the gas environments (O_2 and Ar) and specimen heating were adopted. The temperature was measured at the sample surface with a thermocouple.

III. RESULTS

Figure 1 shows the charging processes during the first and second electron exposure at room temperature. After the first exposure the sample was discharged completely by specimen heating. During the first electron exposure the sample showed an abnormal charging behavior. The charging potential U_c was measured by the shift of the Auger peaks.

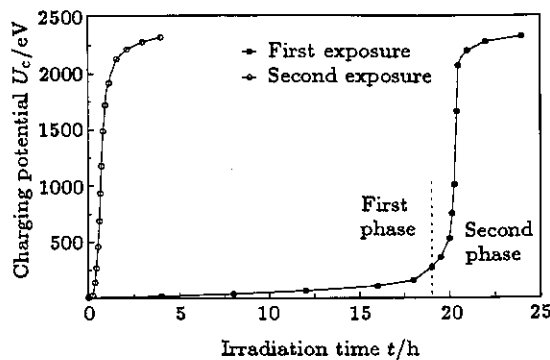


Fig.1. The charging processes during the first and second electron exposures. Before the second exposure the sample has been discharged completely by specimen heating. ($E_p=5$ keV and $\alpha = 30^\circ$).

The surface can be reduced by electron bombard-

ment through ESD. Simultaneously, surface contamination from carbon often takes place. The Auger peaks at 141 and 87 eV are selected to characterize the ESD and the carbon contamination, because the former, being a $\text{Zr}(\text{MNV})$ -transition, can be readily influenced by the surface chemical bonding, and the latter, being a core-core-core transition, is not significantly affected by the surface chemical bonding.

ESD of the surface oxygen and adsorption of the residual gas has been followed during specimen heating without charging occurrence. Figure 2 indicates the change of the 141 eV peak (Zr_{141}) upon the exposure of 5 keV electrons at 250°C . The radiation time is given for each spectrum. The reduced surface gives an additional peak at about 148 eV, which can be collated to metallic zirconium. With desorption of oxygen, adsorption of carbon and carbonation of the surface take place. The "carbide" peak appears at about 145 eV. The energy shift (≤ 3 eV) of the $\text{Zr}(\text{MNN})$ peak can be attributed to the charging effect.

The 6.5×10^{-6} Pa O_2 can completely compensate the electron beam effects at normal incidence of 2.5 keV electrons and at 30° incidence of 3 keV electrons, respectively. The sample keeps stoichiometric and charging free during the lasting radiation for two days. Figure 3 shows the spectra for the 3 keV primary energy at 30° incidence. By contrast, the 1.3×10^{-2} Pa Ar reached a compensation of the charging only up to the primary energy 2 keV at 30° incidence, with transient charging at the beginning of the radiation. Carbon contamination in this Ar atmosphere can be more quickly than in ultrahigh vacuum (UHV). Figure 4 shows the charging processes of the surface during the exposure of 3 keV electrons in 1.3×10^{-2} Pa Ar and in UHV, respectively. The charge potential in 1.3×10^{-2} Pa Ar spontaneously reached a maximum, then it discharges a little. The saturation charging is about 500 eV lower than that in UHV.

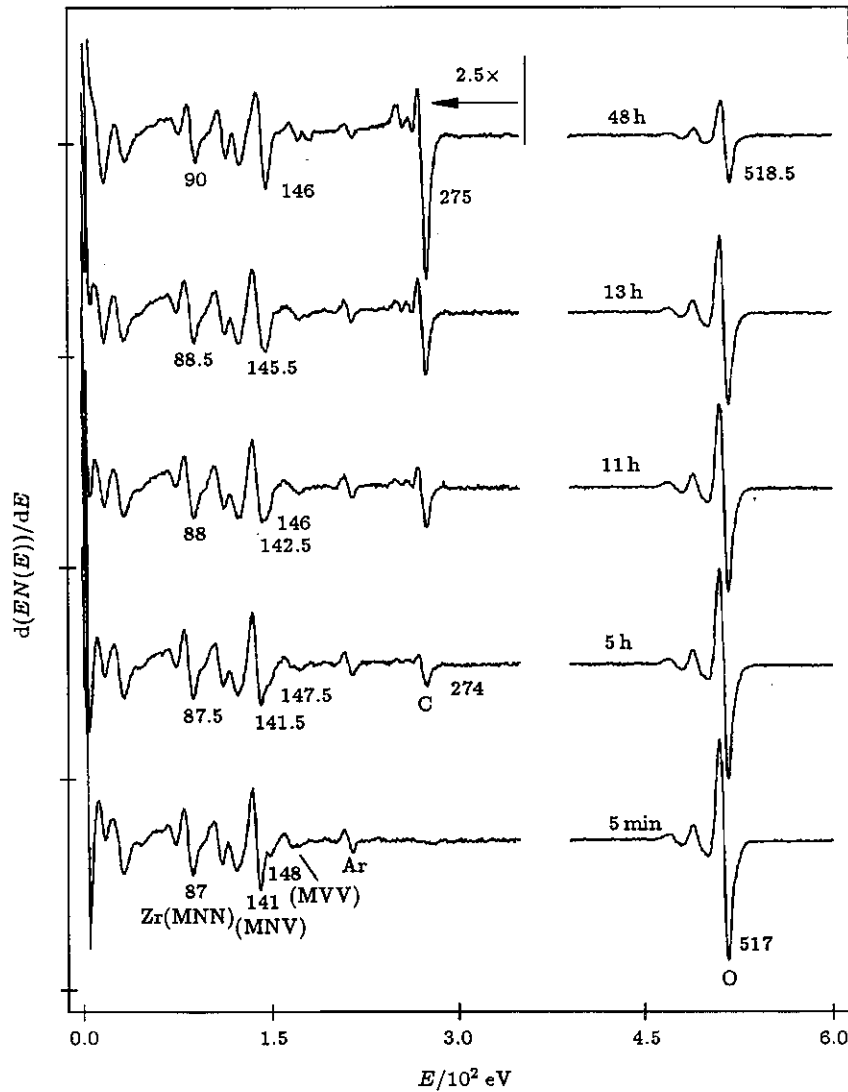


Fig.2. Oxygen desorption and carbon absorption of the surface under bombardment of 5 keV electrons. The peak energies of Zr(MNN) and Zr(MNV) and the irradiation time are indicated for each spectrum. ($\alpha = 30^\circ$ and 250°C).

Specimen heating can eliminate the charging-up of the sample by the primary parameters given in Table 1. Table 2 lists the ratios of the peak intensities obtained in the temperature range from 450°C to 120°C . In the table Zr_{87}/O and C/O are used to indicate oxygen deficiency and carbon contamination of the surface after the electron bombardment for 48 h. The oxygen deficiency and the carbon contami-

nation of the surface depend on the sample temperatures, while at the same temperature they depend in turn on the primary energy. The oxygen desorption and carbon contamination can be reduced by offering an O_2 environment below 6.5×10^{-6} Pa. The spectra from the sample at 350°C in the O_2 atmosphere are given in Figs.5 and 6 for 8 keV and 5 keV, respectively.

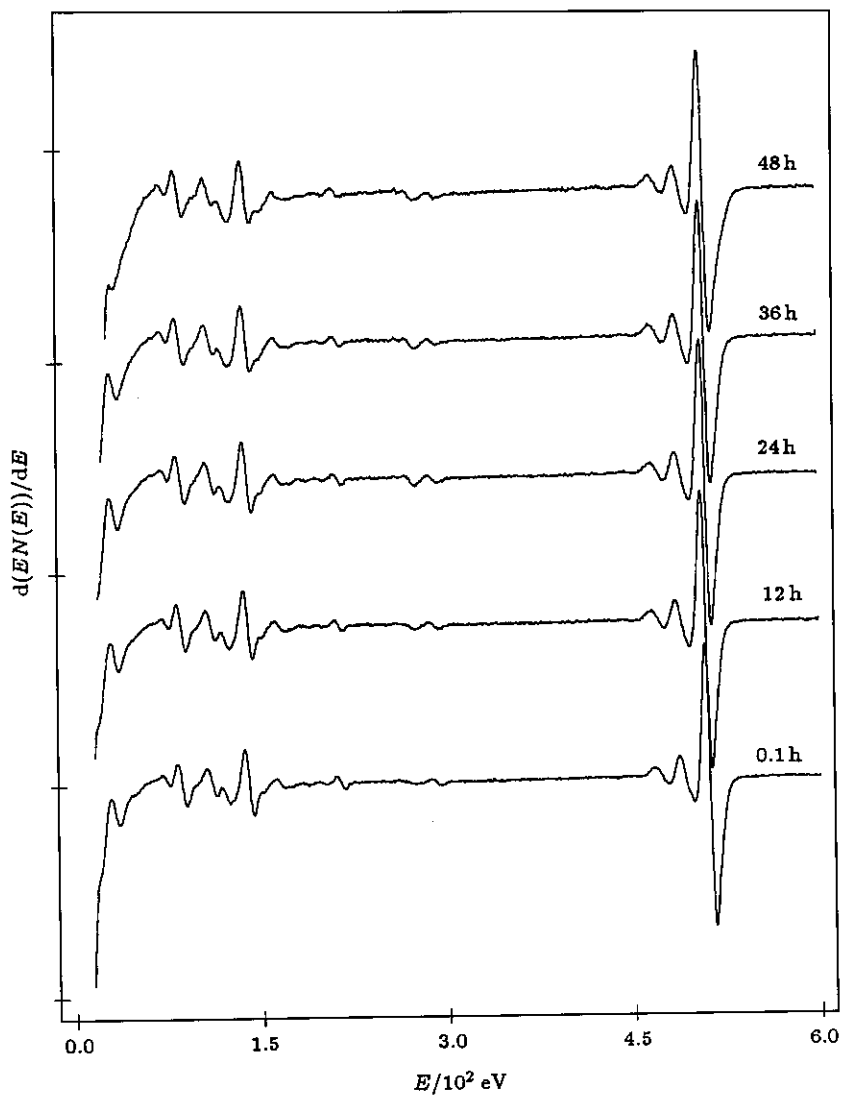


Fig.3. The spectra acquired at 3 keV and 30° incidence in 1.3×10^{-6} Pa O_2 . The irradiation time is given for each spectrum.

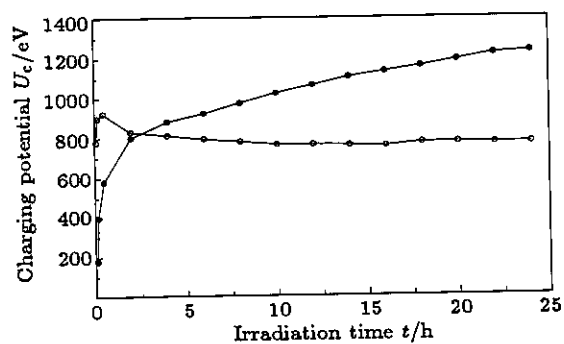


Fig.4. The charging processes in UHV (\bullet) and in 1.3×10^{-2} Pa Ar (\circ) under the 3 keV electron bombardment at 30° incidence.

Table 2. The peak intensity ratios after the electron bombardment for 48 h with specimen heating in UHV.

E_p /keV	$T/^\circ\text{C}$	450	350	250	190	150	120	100
8	Zr ₃₇ /O	0.128	0.149	0.171	0.187	0.211		
	C/O	0.15	0.05	0.223	0.337	0.454	0.527	
	U_c /eV	0	0	2	2	14	64	490
5	Zr ₃₇ /O	0.150	0.157	0.190	0.211	0.217		
	C/O	0.551	0.637	0.662	0.738	0.913	0.951	
	U_c /eV	3	3	3	3	3	40	645

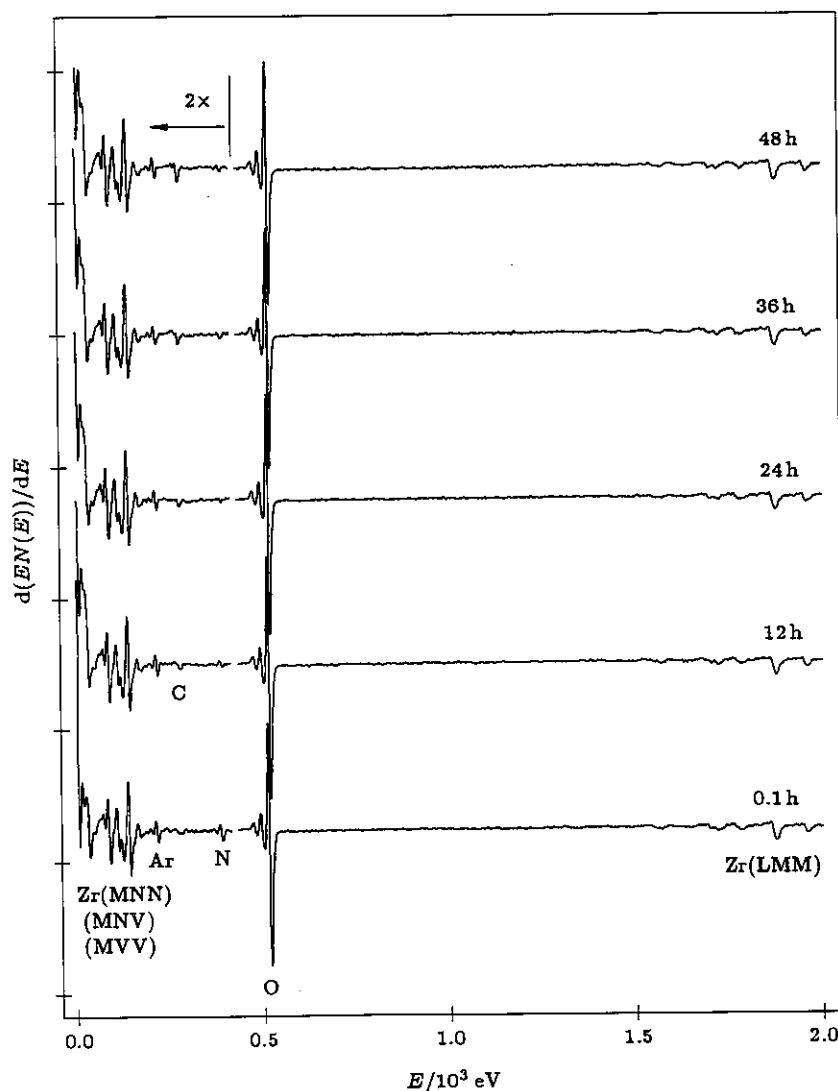


Fig.5. The spectra obtained in O_2 environmental AES ($6.5 \times 10^{-6} \text{ Pa O}_2$) with specimen heating. The irradiation time is given for each spectrum. ($E_p=8 \text{ keV}$, $\alpha = 30^\circ$ and 350°C).

During the radiation of 48 h no charging appears, and the largest C/O ratios are 0.08 for 8 keV and 0.20

for 5 keV. Without an O_2 environment the surface will be strongly reduced and seriously contaminated by

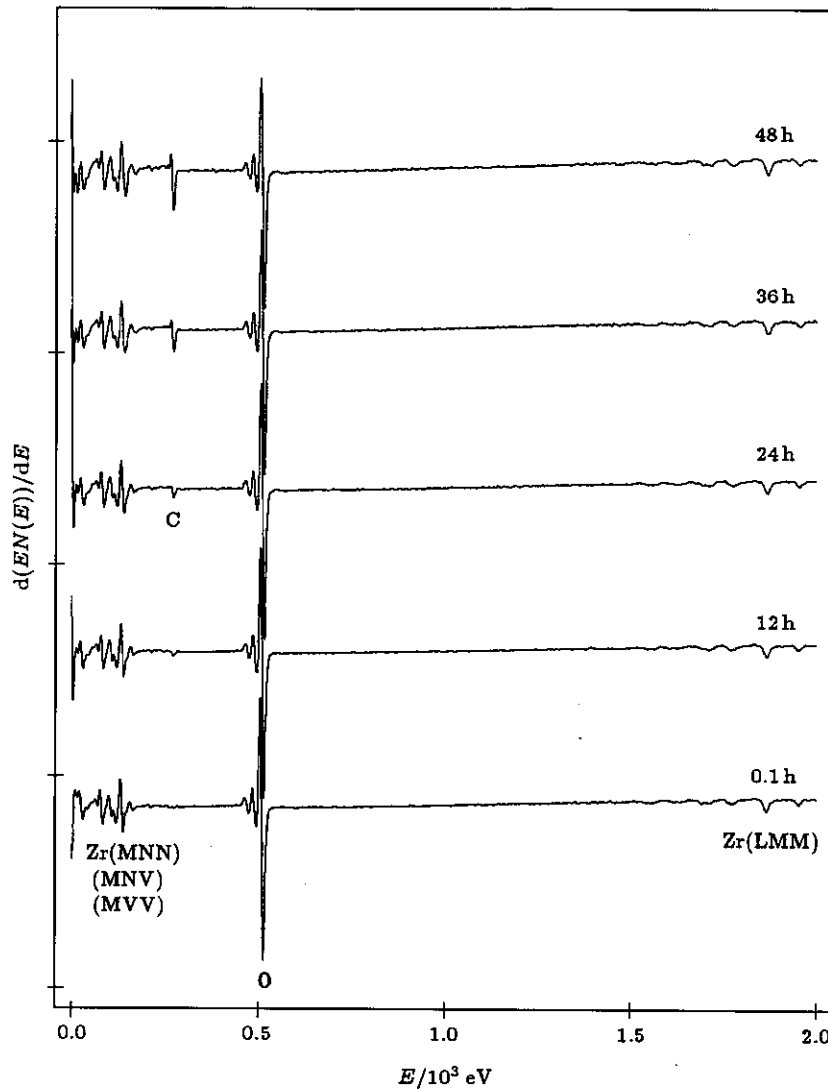


Fig. 6. The spectra obtained during charging compensation by specimen heating in 6.5×10^{-6} Pa O_2 . The irradiation time is given for each spectrum. ($E_p=5$ keV, $\alpha = 30^\circ$ and $350^\circ C$).

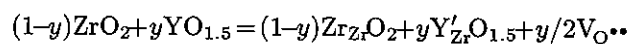
carbon. This can be learnt from Table 2.

IV. DISCUSSION

Morant *et al.*^[2] noted that three different sub-oxides, Zr_2O_3 , ZrO , Zr_2O , and metallic zirconium, can be formed under the bombardment of energetic Ar^+ (3 keV). Axelson *et al.*^[3] estimated that the cross section of ESD of pure ZrO_2 under the bombardment of 3 keV electrons is about 21×10^{-22} cm². From the peak intensities in Fig. 2, the composition of the surface after electron radiation for 48 h is 33.6 at% Zr, 28.1 at% O and 38.3 at% C (a half-quantitative analysis neglecting yttrium in the sample). This result infers that the large part of adsorbed carbon composes the "carbide" on the reduced surface.^[4] Carbon atoms can also permeate through the lattice of YS- ZrO_2 , especially on specimen heating.^[4] This explains why the intensities of the peaks of Zr(MNN) and Zr(MNV) re-

main unchanged (Fig. 2).

ESD and carbon contamination can be reduced in O_2 environmental AES, as a result, the related charging, which is dominant at low primary energy, is reduced (Fig. 3). Besides ESD at the surface, the primary electrons modify the preexisting defects in YS- ZrO_2 , such as oxygen vacancies, which then become capable of charging. In YS- ZrO_2 the yttrium substitutes for the zirconium sites in the lattice. Each Y atom induces a half oxygen vacancy due to the electron neutrality.



Y'_{Zr} indicates yttrium on the zirconium site with a formal charge of -1 , and $V_{O^{\bullet\bullet}}$ indicates a double ionized oxygen vacancy. The sample with 9 mol% Y_2O_3 has a composition of $Zr_{0.82}Y_{0.18}O_{1.91}$, or 4.5% of oxygen vacancies.

Using extended X-ray absorption fine structure (EXAFS) technique, Catlow *et al.*^[5] confirmed that the coordination number of Zr in YS-ZrO₂ is less than 8, but equals to 8 for Y. Furthermore, using electron paramagnetic resonance (EPR), Orera *et al.*^[6] revealed that holes are trapped on oxygen anions adjacent to yttrium cations after exposure of YS-ZrO₂ to X-ray at liquid nitrogen temperature. So a significant population of oxygen vacancies is more likely associated with zirconium cations rather than the yttrium cations. It is also known that Al substitutions for Si sites in SiO₂ acting as trap centers for electrons.^[7] All of the facts suggest that Y ion on the Zr site with a negative charge, as denoted formally Y'_{Zr}, is energetically stable.

The ionized oxygen vacancies are effective trap centers for electrons. Azzoni and Orera^[8,9] identified paramagnetic signals in YS-ZrO₂ after it was exposed to X-ray or UV light, or after it was quenched from temperatures above 900 °C in reducing atmosphere (Ar with 5%H₂). The anisotropy EPR signal, denoted as C-defect ([Zr'^{••}V_O]-center), describes a heptacoordinated Zr anion with a captured electron, and the isotropic EPR signal, denoted as T-defect ([V_O••Zr'^{••}V_O]-center), describes an oxygen ion vacancy with an electron surrounded by four Zr anions. In both cases the electrons are trapped in the d level of Zr ions. Azzoni *et al.*^[9] demonstrated that isolated V_O-centers can also be produced under radiation or by reducing the sample at high temperatures, although it is invisible in EPR.

Primary electrons produce electron-hole pairs along their trajectories and cause ESD of the oxygen at the surface. Electrons and holes can be recombined or captured separately. Oxygen vacancies can compose C-defects and T-defectsc with the lattice Zr ions. As a result, the concentrations of the C-defects and T-defects, which are electron traps^[9], are increased. The hole traps are the variants related to Y'_{Zr}.^[6]

The sample studied has 4.5% oxygen vacancies, which corresponds to a concentration of 10²¹ cm⁻³. The two-phase charging process under the first electron exposure in Fig.1 can be explained as follows: The slower charging at the beginning of the first electron exposure is induced by the radiation damage at the surface, i.e., ESD of oxygen. After a long exposure, the internal electric field of the sample is strong enough to modify the preexisting defects, which become capable of charging. This corresponds to the second strong charging.

The activation energy to cause migration of an oxygen vacancy is about 0.84 eV for 9.4mol%Y₂O₃-ZrO₂^[10] and 0.79 eV for 8mol%Y₂O₃-ZrO₂.^[11] From Solier *et al.*'s arrhenius plot of DC conductivity^[10] and assuming oxygen vacancies being isolated, we derive that the specific resistance of 9.4mol%Y₂O₃-ZrO₂ at room temperature is 6.60 × 10¹⁰ Ω·cm, and that it drops down to 2.31 × 10⁵ Ω·cm at 300 °C. According to Hofmann's criterion, AES-insulators, which charge up during AES, should have resistivity greater than 10⁵ Ω·cm.^[12] Thus, charging-free state can be expected by heating 9mol%Y₂O₃-ZrO₂ up to 300 °C. The C-defects have annealing temperatures in the range of 250–300 °C,^[6] and the captured electrons in the C-defects must be released at around 300 °C. Although the annealing of the T-defects requires a temperature above 430 °C,^[8] the raising of the bulk conductivity of YS-ZrO₂ relaxes the requirements.

The data in Table 2 shows that by raising the sample temperature the ratio of Zr₈₇/O increases and that of O/C decreases, i.e., the oxygen deficiency and the carbon contamination at the surface become smaller. One possible interpretation of the phenomena is that the diffusion of oxygen vacancies increases with raising the sample temperature, so that ESD of oxygen can be partially compensated by the migration of oxygen vacancies. Without noticeable oxygen deficiency, carbon has little possibility to adsorb at the surface. Specimen heating discharges the charged sample, because the captured electrons can be detrapped by thermal activation or compensated by ion conductivity. But if specimen heating is ceased, the sample charges up very quickly again, as indicated in Fig.1. This effect implies that the modified defects do not return to their initial states prior to radiation by annealing at temperatures below 300 °C.

V. SUMMARY

Charging-up of 9mol%Y₂O₃-ZrO₂ under electron bombardment is caused by the radiation damage at the surface due to electron-stimulated desorption, as well as by the preexisting defects, such as oxygen vacancies, which can be modified by electron beam. The charging from the first process is slow and monotonous, the charging related to the second process increases drastically. For reducing the electron beam effect at the surface, the oxygen environment of 6.5 × 10⁻⁶ Pa is more efficient than the Ar of 1.3 × 10⁻² Pa. However, the O₂ environment can eliminate the charging within the limits of primary ener-

gies lower than 3 keV at steep incidence. Although no charging occurs by the specimen heating up to 300 °C, an O₂ environment is necessary to compensate the reduction of the surface oxygen and to inhibit the carbon contamination.

The electron traps related to the oxygen vacancies are suggested to be C-defects and T-defects, which represent heptacoordinated Zr anions and the four coordinated oxygen vacancies, respectively. YS-ZrO₂, as a good solid electrolyte, the captured electrons on the defects can be detrapped by thermal activation or

compensated by ion conduction during the specimen heating. However, the radiation-modified defects cannot heal to their initial states prior to the radiation by annealing below 300 °C.

ACKNOWLEDGMENTS

Financial support by the Deutsche Forschungsgemeinschaft (SFB 180) is gratefully acknowledged. We thank G. Borchardt (Technische Universität Clausthal) for providing us with some of the samples studied.

REFERENCES

- [1] H. S. Guo, W. Maus-Friedrichs and V. Kempter, *Surf. Interface Anal.*, **25**(1997), 390.
- [2] C. Morant, J. M. Sanz and L. Galàn, *Phys. Rev.*, **B45**(1992), 1391.
- [3] K. O. Axelson, K. E. Keck and B. Kasemo, *Appl. Surf. Sci.*, **25**(1986), 217.
- [4] D. L. Cocke and M. S. Owens, *Appl. Surf. Sci.*, **31**(1988), 471.
- [5] C. R. A. Catlow, A. V. Chadwick, G. N. Greaves and L. M. Moroney, *J. Am. Ceram. Soc.*, **69**(1986), 272.
- [6] V. M. Orera, R. I. Merino, Y. Chen, R. Cases and P. J. Alonso, *Phys. Rev.*, **B42**(1990), 9782.
- [7] D. R. Young, D. J. DiMaria, W. R. Hunter and C. M. Serrano, *IBM J. Res. Develop.*, **22**(1978), 285.
- [8] C. B. Azzoni and A. Paleari, *Phys. Rev.*, **B40**(1989), 6518; *Solid State Ion.*, **44**(1991), 267.
- [9] A. E. Hughes, in: "Science of Ceramic Interface II" (Materials Science Monographs 81), edited by J. Nowotny (Elsevier, 1994), p.183.
- [10] J. de D. Solier, M. A. Pérez-Jubinda, A. Dominguez and A. H. Heuer, *J. Am. Ceram. Soc.*, **72**(1989), 1500.
- [11] J. H. Park, "Electronic Transport in Yttria Stabilized Zirconia", Ph. D. Thesis, Marquette University (Milwaukee, Wisconsin, July, 1985).
- [12] S. Hofmann, *J. Electron Spectrosc. Relat. Phenom.*, **59**(1992), 15.